NASA MEMO 6-10-59L

NASA

MEMORANDUM

EXPERIMENTAL INVESTIGATION OF THE HEAT-TRANSFER RATE TO A SERIES OF 20° CONES OF VARIOUS SURFACE FINISHES AT A MACH NUMBER OF 4.95

By Jim J. Jones

Langley Research Center
Langley Field, Va.

NATIONAL AERONAUTICS AND SPACE ADMINISTRATION
WASHINGTON
June 1959

ERRATA

NASA MEMO 6-10-59L

By Jim J. Jones
June 1959

Pages 23 to 26: In figures 7(a), 7(b), 7(c), and 7(d), the values for R_x' in the abscissa scale should be changed as follows:

10^6 should be 10^5

10^7 should be 10^6

10^8 should be 10^7

Issued 10-16-61

NASA-Langley, 1961

NATIONAL AERONAUTICS AND SPACE ADMINISTRATION

MEMORANDUM 6-10-59L

EXPERIMENTAL INVESTIGATION OF THE HEAT-TRANSFER RATE TO A SERIES OF 20° CONES OF VARIOUS SURFACE FINISHES AT A MACH NUMBER OF 4.95

By Jim J. Jones

SUMMARY

The heat-transfer rates were measured on a series of cones of various surface finishes at a Mach number of 4.95 and Reynolds numbers per foot varying from 20×10^6 to 100×10^6. The range of surface finish was from a very smooth polish to smooth machining with no polish (65 microinches rms).

Some laminar boundary-layer data were obtained, since transition was not artificially tripped. Emphasis, however, is centered on the turbulent boundary layer. The results indicated that the turbulent heat-transfer rate for the highest roughness tested was only slightly greater than that for the smoothest surface. The laminar-sublayer thickness was calculated to be about half the roughness height for the roughest model at the highest value of unit Reynolds number tested.

INTRODUCTION

Since hypersonic vehicles may encounter flight conditions such that a large portion of the vehicle's surface will be exposed to the heating rate of a turbulent boundary layer, it becomes of interest to know what surface finish is required to avoid increasing the heating rate excessively. In references 1 and 2, for instance, it was found that at supersonic speeds the effects of surface finish, or distributed roughness, on skin friction were similar to those found for the incompressible case by Nikuradse (ref. 3) some time ago. That is, if the roughness is small compared with the laminar-sublayer thickness, the turbulent skin-friction coefficient is the same as for smooth walls. As the average height of the roughness elements becomes of the same order as the laminar-sublayer thickness the skin friction departs from the curve for the smooth wall and very sizable increases in skin friction may result. If some modified Reynolds analogy holds true for rough surfaces, the heat transfer would

exhibit effects of roughness similar to those of the skin friction. However, very little information is available on the heat-transfer rate to rough surfaces, nor has the Reynolds analogy been verified for surfaces with roughness.

It is assumed herein that very rough surfaces are avoided as a matter of course in the fabrication of high-speed vehicles and that the range of principal interest extends from a polished surface to a surface which is obtained by ordinary machining with no polish, or the finish of stock rolled sheet metal. An ordinary smooth-machined surface is taken to be that designated by the SAE symbol $\overset{63}{\checkmark}$—, which has a root-mean-square roughness height of about 63 microinches. This range covers the expected surface finishes of most aircraft exteriors, with the exception of joints, protrusions, and so forth, which represent a separate category of roughness and are not considered herein.

In the present investigation, a series of cones of varying surface finish were tested at a Mach number of 4.95 and heat-transfer measurements were made. For the particular conditions (Mach number, Reynolds number, and wall-to-stream temperature ratio) at which the models were tested, the ratio of height of the average roughness element to the calculated laminar-sublayer thickness had an upper limit of about 2 or 3. Therefore, the skin-friction coefficient would be expected to be only slightly greater than for the smoothest model and, assuming that the Reynolds analogy holds, the effect of roughness on heat-transfer rate should also be small.

While the unit Reynolds number encountered in flight would not be as high as that at which the tests were run, the boundary-layer cooling rate would, in many cases, be much greater, especially for very high flight speeds. Since the cooling has a thinning effect on the laminar sublayer, the tests should be in the range of practical interest.

SYMBOLS

A_{av}	average skin area, equal to reference volume divided by skin thickness
A_w	external skin reference area
c_p	specific heat at constant pressure, Btu/(slug)($^\circ$R)
c_w	heat capacity of wall material, Btu/(lb)($^\circ$R)
h	heat-transfer coefficient, Btu/(sec)(sq ft)($^\circ$R)

h_m	measured heat-transfer coefficient uncorrected for normal conduction effects, Btu/(sec)(sq ft)(^oR)
k	roughness height, ft unless otherwise indicated
M	Mach number
m	reference mass of skin
N_{St}	Stanton number, $h/\rho c_p V$
p/p_∞	static pressure on cone divided by free-stream static pressure
Q	quantity of heat transferred per unit time, Btu/sec
R_k	roughness Reynolds number, $\rho_k V_k k/\mu_k$
R_x	Reynolds number based on x, $\rho V x/\mu$
R_{x_t}	Reynolds number based on x_t, $\rho V x_t/\mu$
T	temperature, ^oR
T_r	recovery (or adiabatic wall) temperature, ^oR
t	skin thickness, ft
V	flow velocity, ft/sec
v_*	friction velocity, ft/sec
x	surface distance from apex, ft unless otherwise indicated
x_t	surface distance from fictitious starting point of turbulent boundary layer, ft
β	cone half-angle
δ_l	laminar-sublayer height
μ	viscosity, slugs/(ft)(sec)
ν	kinematic viscosity, μ/ρ, ft^2/sec
ρ	density of air, slugs/cu ft

ρ_w specific weight of skin material, lb/cu ft

τ time, sec

Subscripts:

e local conditions external to boundary layer

k conditions at distance k from surface

w wall or skin values

A prime denotes conditions evaluated at reference temperature.

MODELS AND TEST APPARATUS

A cone was selected as the model shape for this investigation because it was desired to conduct the tests on a body having zero streamwise pressure gradient. A sketch of the model configuration is shown in figure 1. The models were constructed of 17-4 PH stainless steel and had a skin thickness of 0.060 inch. The nose radius on all models was about 0.0005 inch.

Four heat-transfer models of varying roughness and one pressure model were constructed. The pressure model was polished to about 15 microinches. The surface roughness of the heat-transfer models was controlled by varying the amount of polishing after machining. The smoothest model (model 1) was carefully polished until the average roughness was not greater than 2 microinches, as measured with an interference microscope. In figure 2, sample interference-microscope pictures are shown for models 1 and 2. For the wavelength of light used, a fringe shift equal to the local fringe spacing represents a change in surface height of 10.75 microinches. The fringes are not evenly spaced because the surface is curved. Note that there are dents and scratches quite a bit deeper than the average roughness level, but they do not weigh heavily in determining an average roughness height because of their scarcity. Model 2 had an average roughness height of about 7 microinches. Models 3 and 4 were too rough to allow measurement with the interference microscope; therefore, a profilometer, which measures the root-mean-square roughness height from the mean line, was used. The profilometer indicated a root-mean-square roughness height of 15 microinches for model 3 and 65 microinches for model 4. In order to determine the average peak-to-valley height from the root-mean-square height, it is necessary to know the shape of the roughness. If the shape were sawtooth the ratio of total height to root-mean-square height would be $\sqrt{12}$; if the shape were sinusoidal the ratio would be $\sqrt{8}$. Actually

it was neither, of course. Inspection of model 4 under a microscope indicated that the roughness elements tended to have rounded peaks and V-shaped valleys, with an average spacing of about 0.005 inch. Although knowledge of the form of the roughness elements might help in interpreting the present results, this investigation is intended as a study of the effects of typical machined surfaces rather than of a particular size or shape of roughness element.

No scratches, dents, or abrasions were detected on any of the models as a result of the tests.

The heat-transfer models had iron-constantan thermocouples welded to the inner surface of the skin at the stations indicated in figure 1. The pressure-distribution model had flush orifices installed at the same stations.

The tests were conducted in the Langley Gas Dynamics Branch in an axisymmetric Mach number 4.95 blowdown jet which had a 9-inch-diameter test section. The stagnation temperature of all tests was near 860° R. Each model was tested at stagnation pressures of 500, 1,000, 1,500, 2,000, and 2,500 pounds per square inch. The corresponding free-stream Reynolds number range was 15×10^6 to 75×10^6 per foot. (Or, based on inviscid conditions at the surface of the cone, the Reynolds number range was 20×10^6 to 100×10^6 per foot.) The ratio of wall temperature T_w to local stream temperature T_e was about 3 for all tests.

For the heat-transfer runs the jet was started and brought to steady operating conditions with the model outside the test section. Then a plate which covered the test-section opening was lowered and the test-section door, with the model mounted on it, was injected by a pneumatic actuator. It has been determined in another experiment that approximately 0.05 second elapses from the instant the model first begins to move into the stream until it reaches its test position and steady flow is established.

The model remained in the airstream only 3 to 5 seconds in most instances and then was retracted. It was then cooled down to approximately 75° F before the succeeding run. The data were evaluated at the instant the model had been in the flow 1 second. The increase in the model temperature at this time was about 30° F. A brief account of the procedure for reducing the temperature-time records of the heat-transfer data is included in the appendix.

The pressure-distribution model remained in its test position throughout the run and thus was very near adiabatic-wall temperature.

The angle of attack of all tests was 0° ± 1°.

RESULTS AND DISCUSSION

Pressure Distribution

The experimentally found distribution of static pressure along the cone surface is presented in figure 3. The ray of the cone along which the orifices were located was oriented with respect to the tunnel in the same manner as the thermocouple locations on the heat-transfer model. Rotation of the model on its axis produced nearly identical distributions. The decreasing pressure near the rear of the model was apparently a tunnel effect. For convenience the model was mounted somewhat rearward of the original test locations, and tunnel calibration data are not available for this location. While the pressure along the cone is not as uniform as is desirable, the pressure gradient is favorable and is not believed to affect the heat-transfer data seriously. The local stream Mach numbers indicated in figure 3 are based on the assumption of isentropic flow behind a Mach number 4.95 conical shock wave.

Heat Transfer

The heat-transfer data for the four models are shown in figure 4, where the Stanton number N_{St} is plotted against Reynolds number R_x. The air properties were evaluated for stream conditions just outside the boundary layer. The Prandtl number was taken as a constant, 0.71. The laminar and turbulent recovery factors, which were not measured experimentally, were assumed to be equal to the square root and cube root, respectively, of the Prandtl number. The turbulent recovery factor was assumed for data in the transition region. Figure 4 also shows Van Driest's analytical relations for comparison (ref. 4). The laminar heating rate is predicted very well by the theoretical curve, but the turbulent data consistently show lower heating rates than the theoretical values. It appears that the roughest model (model 4) had a slightly higher turbulent heating rate than the other models, but the apparent increase was of the same order as the scatter of the data.

A wholly turbulent boundary layer would have been preferable for comparison with turbulent theory. Since transition was not artificially induced near the apex in these tests, however, the boundary layer was, in general, of mixed type, with varying location of the transition point. For this reason a fictitious leading edge for a wholly turbulent boundary layer has been calculated, with the momentum thickness set equal to that of the calculated laminar boundary layer at the observed transition point. In figure 5, the Stanton number for the turbulent portions of the data for models 1 and 4 is presented as a function of the Reynolds number based on x_t, the distance from the fictitious

leading edge. The results in this form are perhaps somewhat more consistent for various values of unit Reynolds number. However, since R_{x_t} is always less than R_x, the data are farther from the theoretical curve. Figure 5(b) indicates that no critical roughness size has been reached; that is, the data do not diverge at some point from an $(R_x)^{-0.2}$ relation.

It is now pertinent to consider the thickness of the laminar sublayer in the turbulent boundary layer as compared with the height of the roughness elements. In figure 6 the calculated laminar-sublayer thickness for model 4 is presented. This thickness was computed by using the relation

$$\delta_l = 5\frac{\nu}{v_*}$$

(See ref. 5.) The temperature at the top of the sublayer was assumed to be equal to the wall temperature for this calculation.

In order to compare the laminar-sublayer thickness with the roughness size, it is necessary to convert the root-mean-square roughness size to the total height, peak-to-valley. For model 4, where the root-mean-square roughness height was 65 microinches, the peak-to-valley height would be about 225 microinches if a sawtooth profile is assumed, and about 185 microinches for a sine-wave profile. Thus, for the highest unit Reynolds number of the investigation, the laminar sublayer was about one-half the average roughness height. While some effect on heat transfer might be expected for roughness of this size, no large increase would be anticipated.

The heat-transfer data have also been reduced on a T' basis; that is, the air properties were evaluated at a reference temperature T', where

$$T' = T_e + 0.5(T_w - T_e) + 0.22(T_r - T_e)$$

(See ref. 6.) The resulting parameters N_{St}' and R_x' are used to present the data in figure 7. The agreement of these data with the classical curves for incompressible flow is very similar to the agreement of the data based on T_e with Van Driest's relations (fig. 4).

Effect of Roughness on Transition

It is evident in figure 4 that the location of boundary-layer transition is nearly constant for models 1 to 3, but that the roughness of model 4 has promoted earlier transition. Without knowledge of the size of the largest roughness elements on model 4, however, it is difficult to interpret the present data.

For an order-of-magnitude estimate, the largest roughness elements are assumed to be 250 microinches high. The roughness Reynolds number R_k varies in a manner similar to the following sketch:

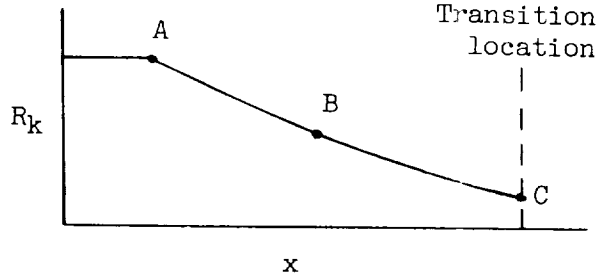

The lowest unit Reynolds number for which an appreciable transition shift was observed was 20×10^6 per foot. (See fig. 4(d).) At point A, where the roughness-element height is equal to the boundary-layer thickness, R_k is then about 400. At point B, where the roughness height is equal to the top of the linear portion of the velocity profile, $R_k \approx 53$. At the transition point C, the value of R_k is about 2.

The roughness Reynolds number of 400 at point A is slightly smaller but of the same order as the roughness Reynolds number found in reference 7 to be critical for sandpaper-type roughness at low speeds. However, in the investigation of reference 7, the lowest values of critical Reynolds number (about 600) occurred only when the roughness element was submerged in the linear-velocity portion of the boundary layer, such as point B. It should be pointed out that in reference 7 the criterion for determining the critical value of R_k was the detection of turbulent bursts by means of a hot-wire anemometer, whereas the present criterion is a shift in the location of transition as determined from the heat-transfer data.

CONCLUDING REMARKS

An investigation has been made at a Mach number of 4.95 to study the effects of surface roughness on the heat-transfer rate to cones

having roughness levels up to 65 microinches rms. The range of Reynolds number per foot was from 20×10^6 to 100×10^6, based on local stream conditions. Although the average roughness height was, for the extreme case, about 2 to 3 times the thickness of the laminar sublayer, the increase in the turbulent heat-transfer rate was small, and of the same order as the data scatter.

The heating rate could be predicted about equally well by the method of Van Driest (ref. 4) or by using the classical incompressible relations and evaluating the gas properties at a reference temperature T'. Both methods tended to overestimate the turbulent heating rate.

Langley Research Center,
National Aeronautics and Space Administration,
Langley Field, Va., March 19, 1959.

APPENDIX

DATA REDUCTION

The thermocouples were connected to an 18-channel recording oscillograph. As was mentioned previously, the model, which was initially at room temperature, was immersed suddenly in the flow and allowed to remain there for a short time. The data were reduced by reading the slope $dT/d\tau$ of each thermocouple and its temperature T for the instant when the model had been in the tunnel 1 second. The oscillograph gain and record speed were adjusted so that the slope of the traces was about 45°, the optimum value for reading accuracy.

Now if the temperature of the thermocouple represented the average temperature of an element of the model skin having mass m, external area A_w, and heat capacity c_w, the heat-transfer rate per unit area would be given by

$$\frac{Q}{A_w} = \frac{mc_w}{A_w} \frac{dT}{d\tau} \tag{1}$$

if it is assumed that no heat is lost to the backing material and that lateral conduction is negligible. The heat-transfer coefficient would be

$$h = \frac{Q}{A_w} \frac{1}{T_r - T_w}$$

However, a finite temperature gradient exists normal to the skin surface, and since the thermocouple is attached to the inner surface of the skin it reads a temperature which is always lower than the average temperature (since heat is flowing into the model skin). For the models tested, the correction can be approximated by

$$\frac{h}{h_m} = 1 + 0.65h_m$$

where h_m is the measured value of the heat-transfer coefficient. This ratio h/h_m never exceeds 1.04 for the data presented. This normal-conduction correction is discussed in more detail in reference 8.

It can be seen from equation (1) that the ratio of the mass of an element of the skin to its external area m/A_w must be evaluated. This can be expressed as $\rho_w A_{av} t_w / A_w$, where A_{av} is an average area which, when multiplied by the skin thickness t_w, gives the volume of an element having external area A_w. For a flat plate of uniform thickness the ratio A_{av}/A_w would, of course, be 1. The expression for a cone of uniform wall thickness is

$$\frac{A_{av}}{A_w} = 1 - \frac{t_w}{2x \tan \beta}$$

Since, at the instant for which the data were evaluated, the skin temperature had not varied greatly from its initial value, the temperature gradients were small and therefore longitudinal conduction effects were neglected. In reference 9, for instance, the longitudinal conduction effect was found to be less than ±2 percent for similar tests.

A check showed that negligible changes in the value of the heat-transfer coefficient h occurred when the data were evaluated at other times (1/2 second, 2 seconds, and 3 seconds).

The data are presented in terms of the Stanton number

$$N_{St} = \frac{h}{\rho c_p V} = \frac{\frac{Q}{A_w}}{\rho c_p V (T_r - T_w)}$$

where the laminar and turbulent recovery factors were assumed to be equal to the square root and cube root, respectively, of the Prandtl number. The turbulent recovery factor was used for the data in the transition region.

REFERENCES

1. Czarnecki, K. R., Robinson, Ross B., and Hilton, John H., Jr.: Investigation of Distributed Surface Roughness on a Body of Revolution at a Mach Number of 1.61. NACA TN 3230, 1954.

2. Sevier, John R., Jr., and Czarnecki, K. R.: Investigation of Effects of Distributed Surface Roughness on a Turbulent Boundary Layer Over a Body of Revolution at a Mach Number of 2.01. NACA TN 4183, 1958.

3. Nikuradse, J.: Laws of Flow in Rough Pipes. NACA TM 1292, 1950.

4. Van Driest, E. R.: The Problem of Aerodynamic Heating. Aero. Eng. Rev., vol. 15, no. 10, Oct. 1956, pp. 26-41.

5. Schlichting, Hermann (J. Kestin, trans.): Boundary Layer Theory. McGraw-Hill Book Co., Inc., 1955, p. 407.

6. Eckert, Ernst R. G.: Survey on Heat Transfer at High Speeds. WADC Tech. Rep. 54-70, U. S. Air Force, Apr. 1954.

7. Von Doenhoff, Albert E., and Horton, Elmer A.: A Low-Speed Experimental Investigation of the Effect of a Sandpaper Type of Roughness on Boundary-Layer Transition. NACA Rep. 1349, 1958. (Supersedes NACA TN 3858.)

8. Trimpi, Robert L., and Jones, Robert A.: Transient Temperature Distribution in a Two-Component Semi-Infinite Composite Slab of Arbitrary Materials Subjected to Aerodynamic Heating With a Discontinuous Change in Equilibrium Temperature or Heat-Transfer Coefficient. NACA TN 4308, 1958.

9. Jack, John R., and Diaconis, N. S.: Heat-Transfer Measurements on Two Bodies of Revolution at a Mach Number of 3.12. NACA TN 3776, 1956.

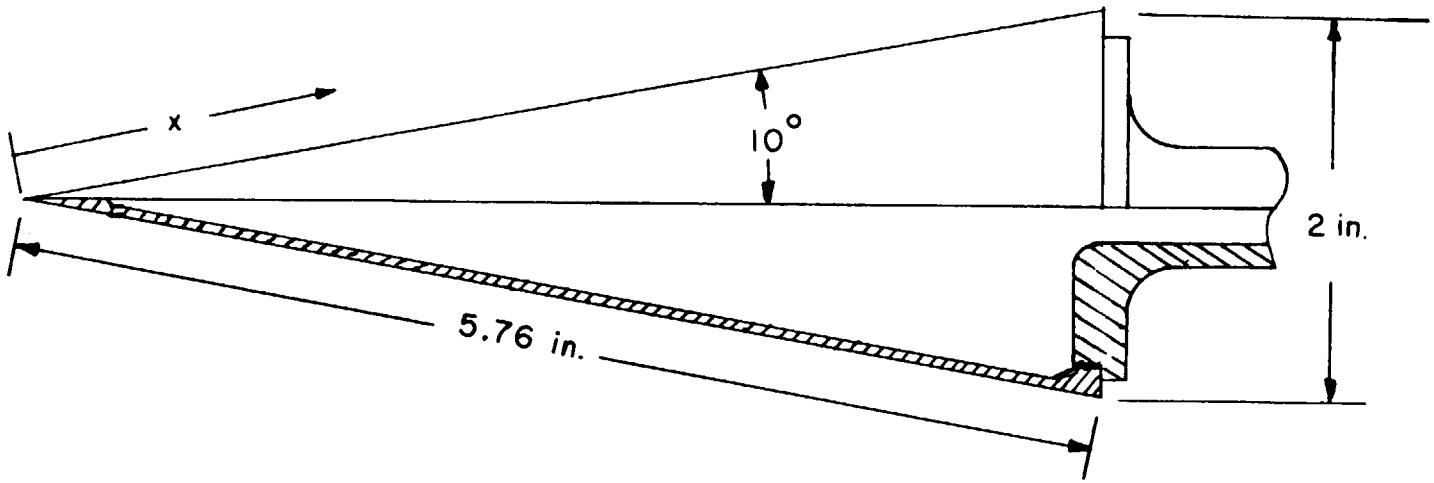

x locations of thermocouples and orifices, inches

1.0	3.75
1.5	4.0
2.0	4.25
2.5	4.5
3.0	4.75
3.25	5.0
3.5	5.25

Figure 1.- Sketch of model configuration.

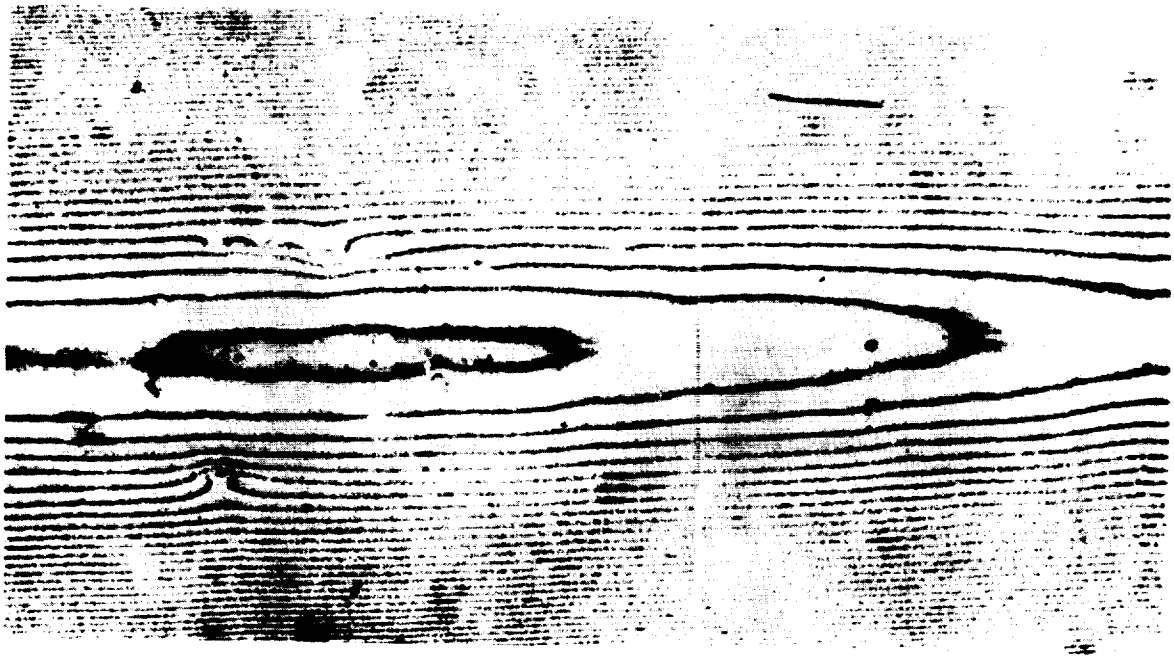

(a) Model 1.

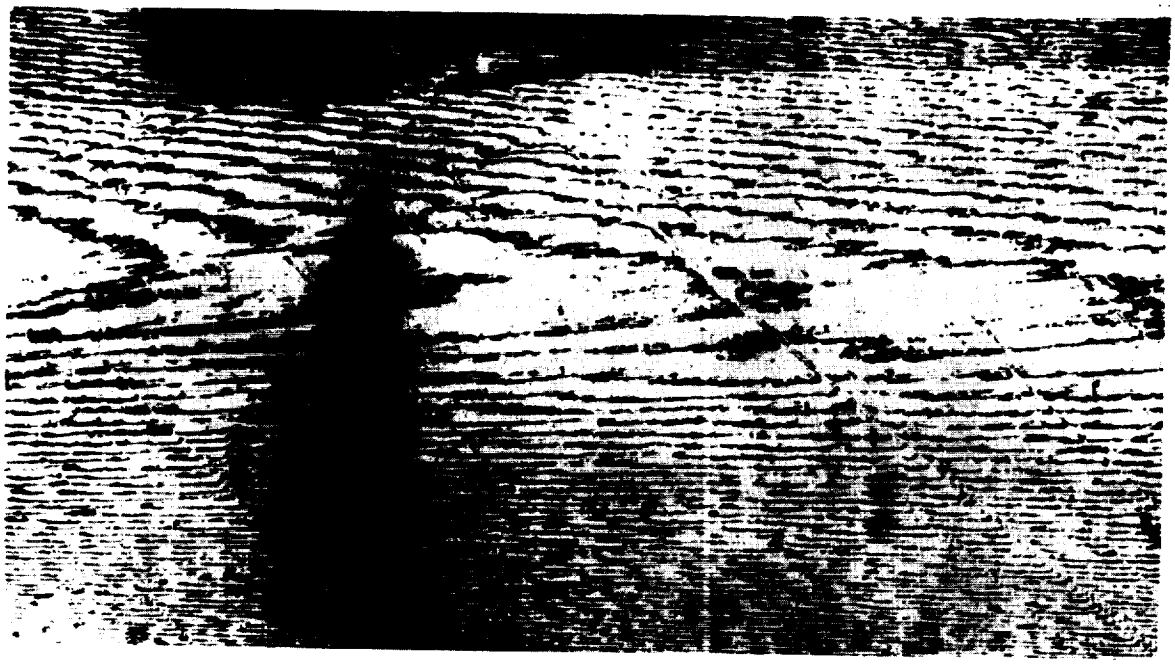

(b) Model 2. L-59-1901

Figure 2.- Interference-microscope pictures of the surface of two of the models.

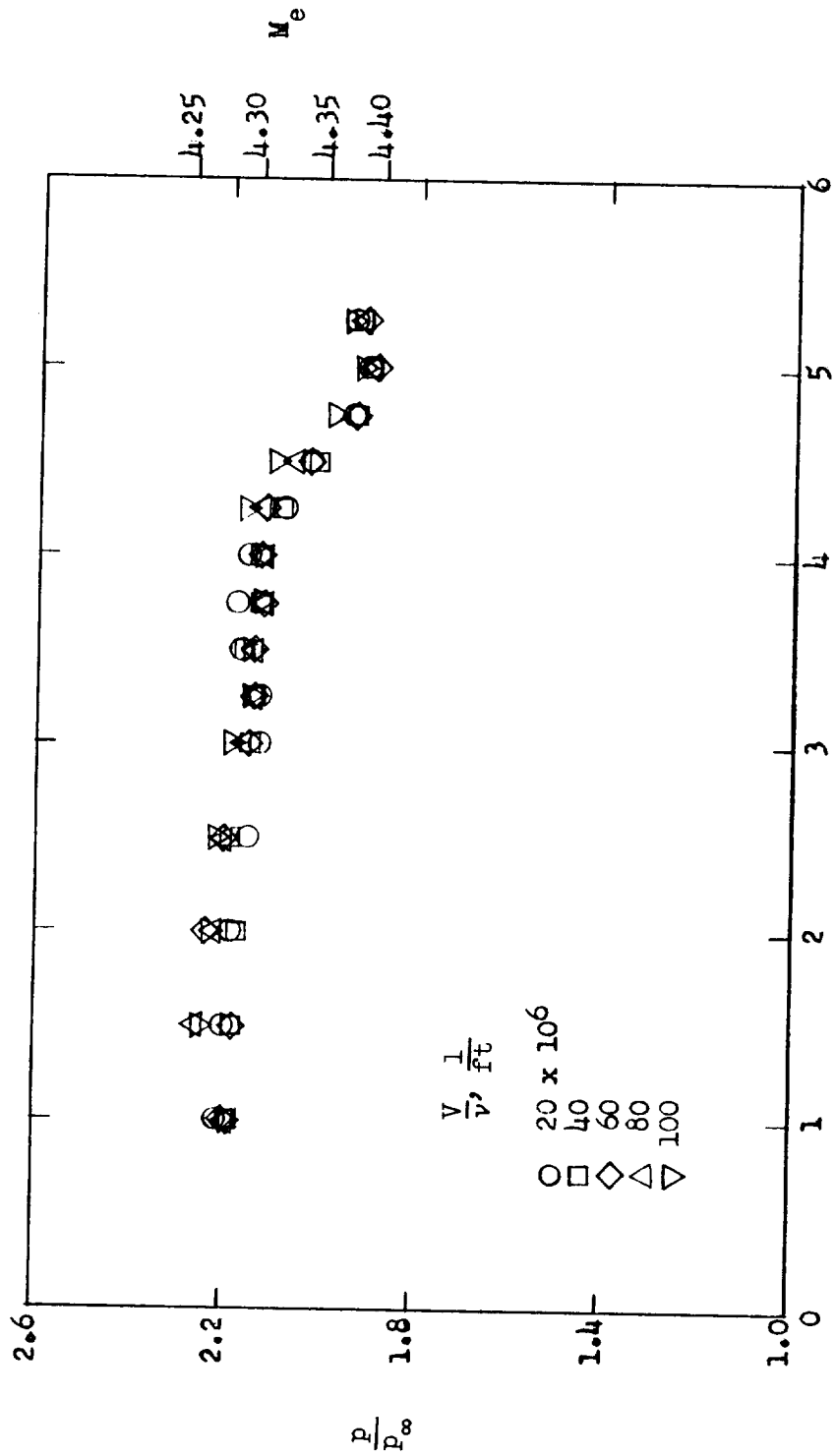

Figure 3.- Pressure distribution along the cone surface.

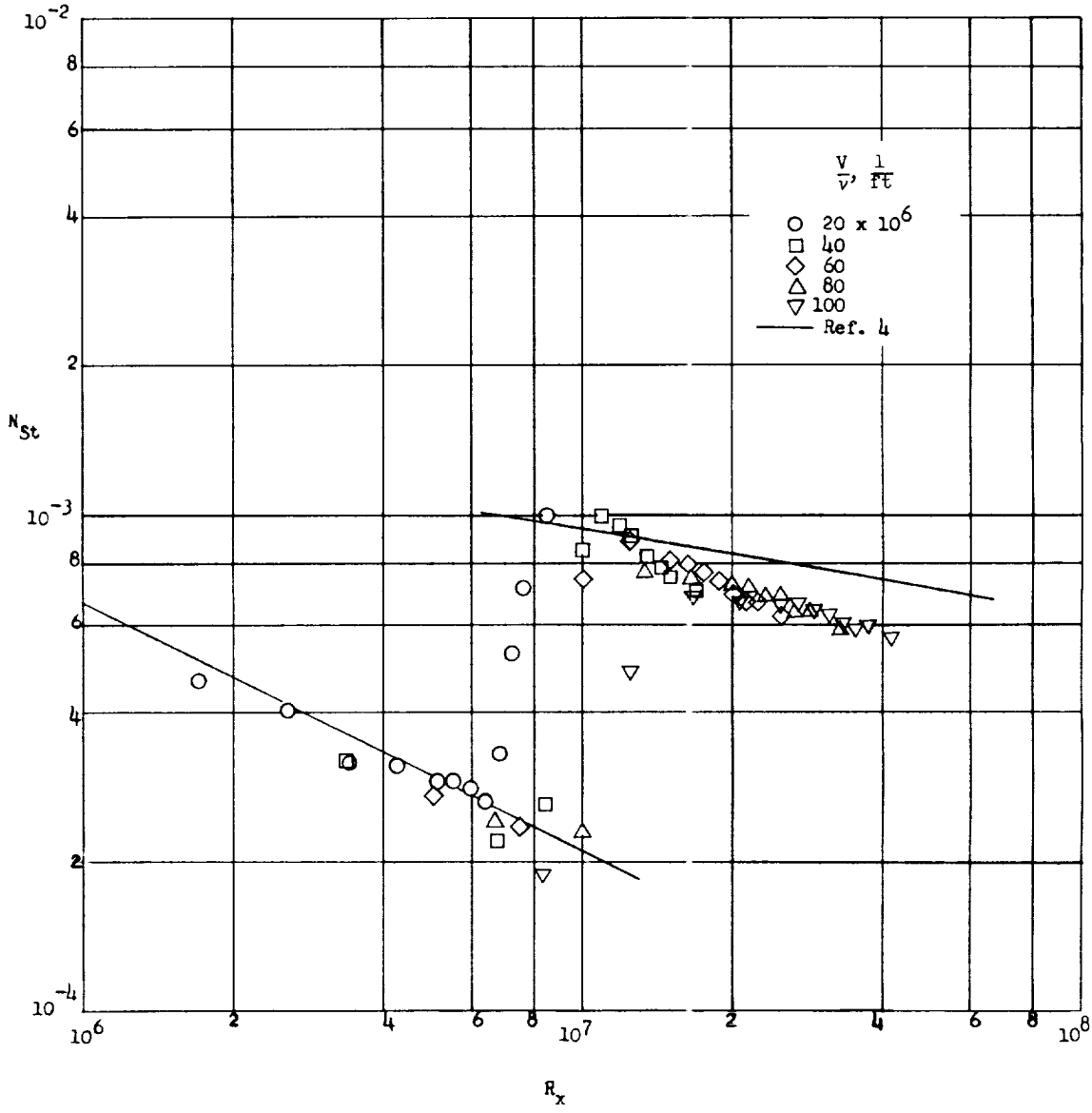

(a) Model 1.

Figure 4.- Heat-transfer data based on local stream conditions.

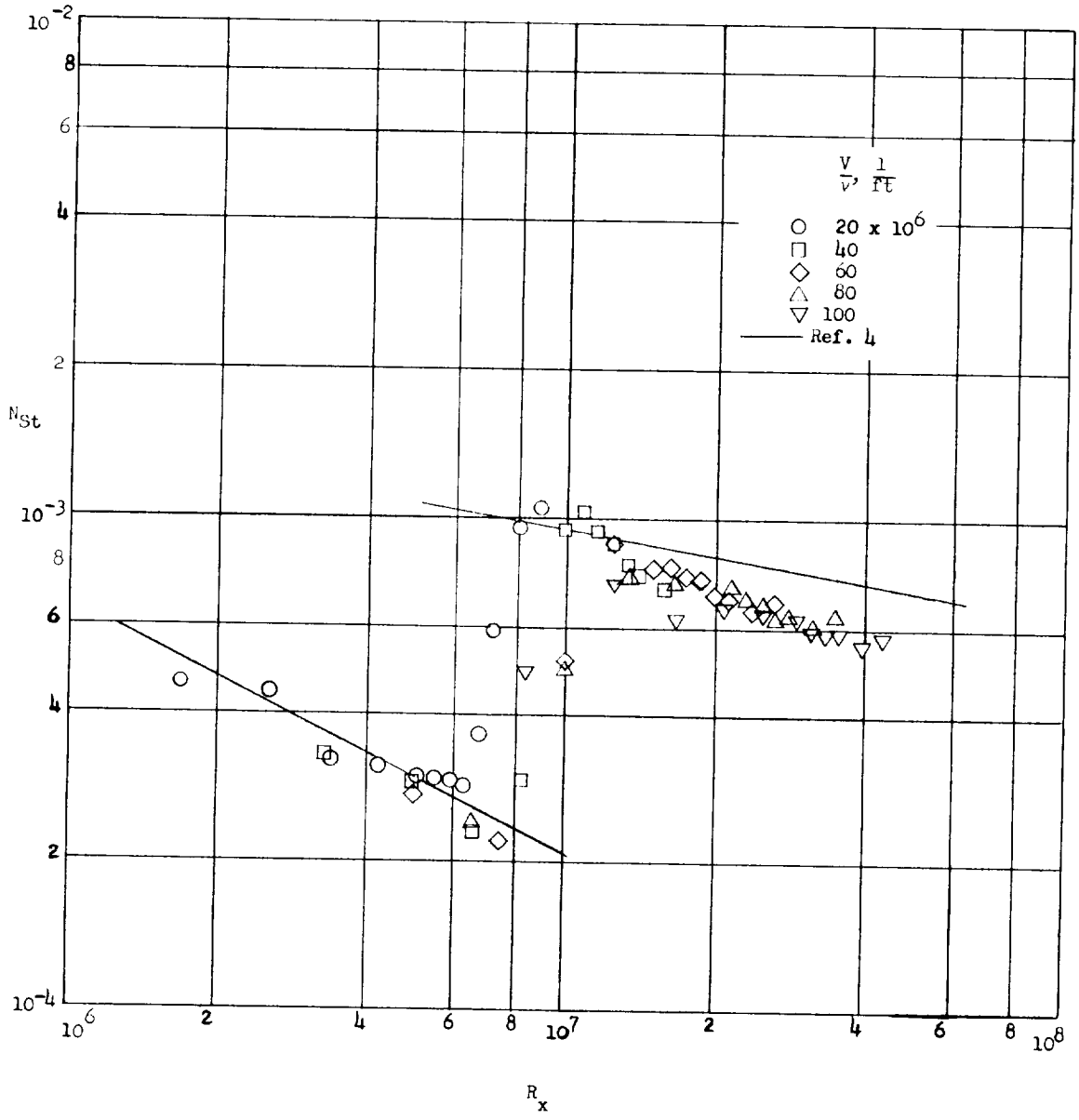

(b) Model 2.

Figure 4.- Continued.

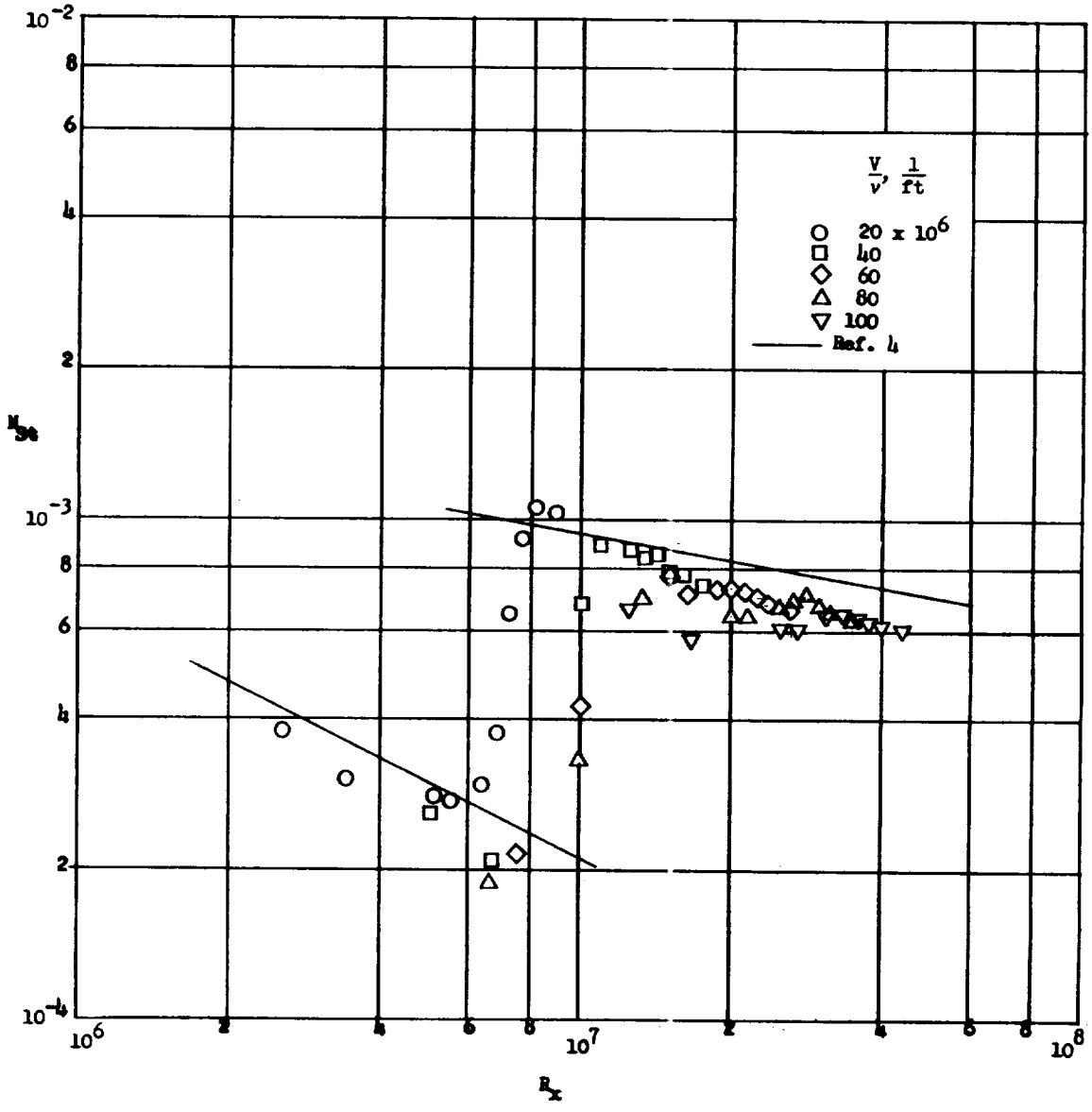

(c) Model 3.

Figure 4.- Continued.

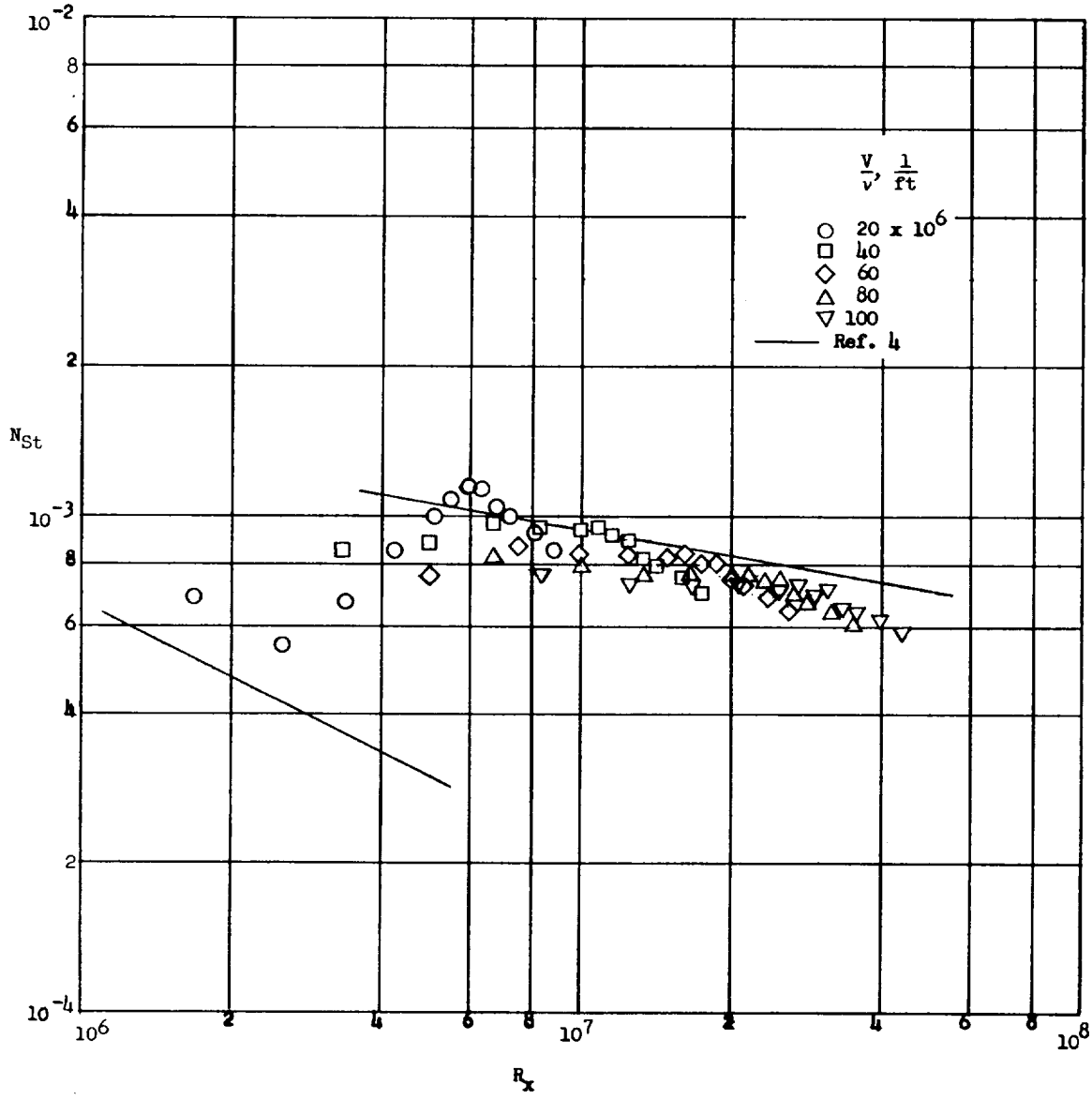

(d) Model 4.

Figure 4.- Concluded.

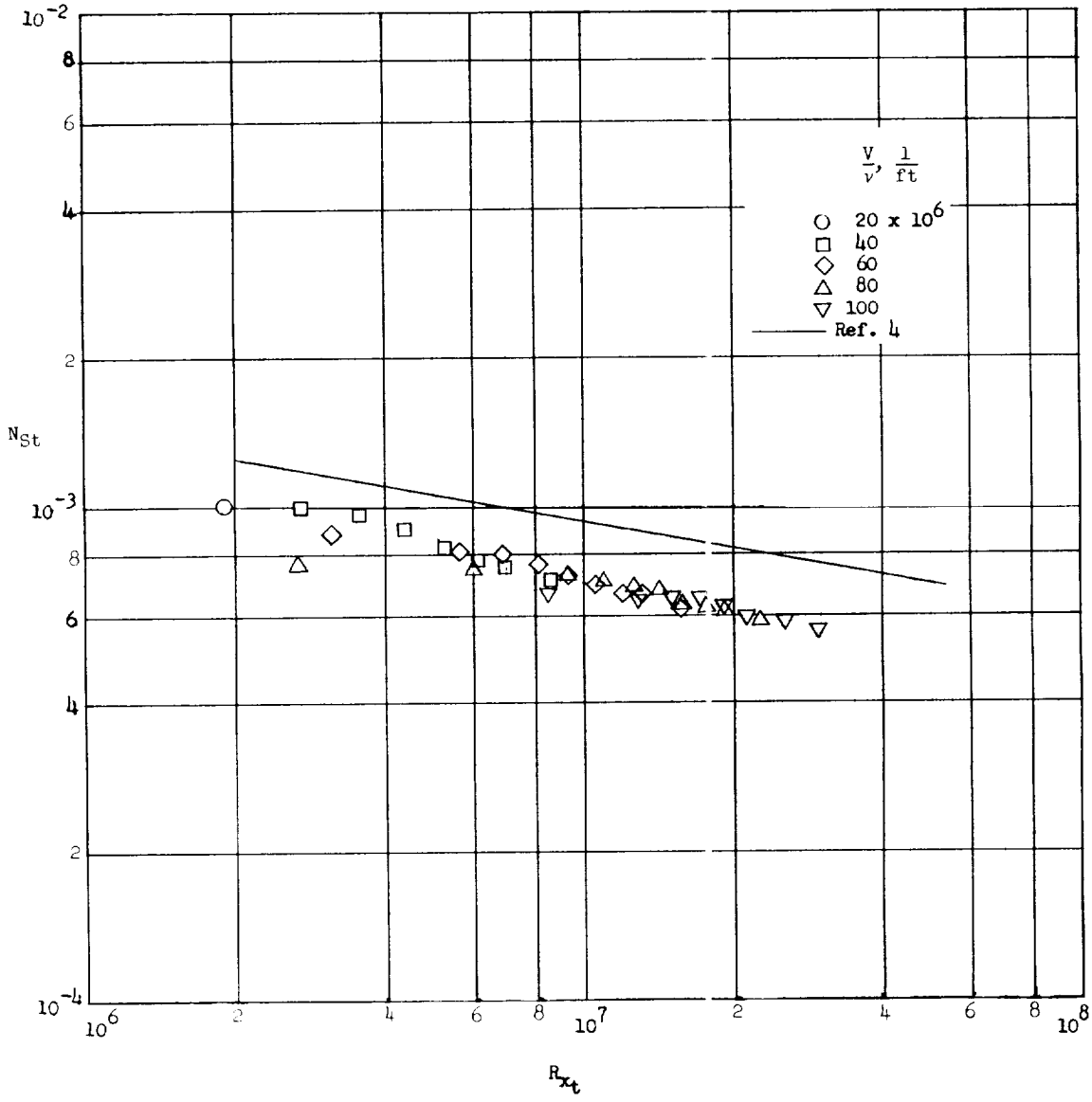

(a) Model 1.

Figure 5.- Stanton number as a function of Reynolds number based on x_t for the turbulent portion of the data.

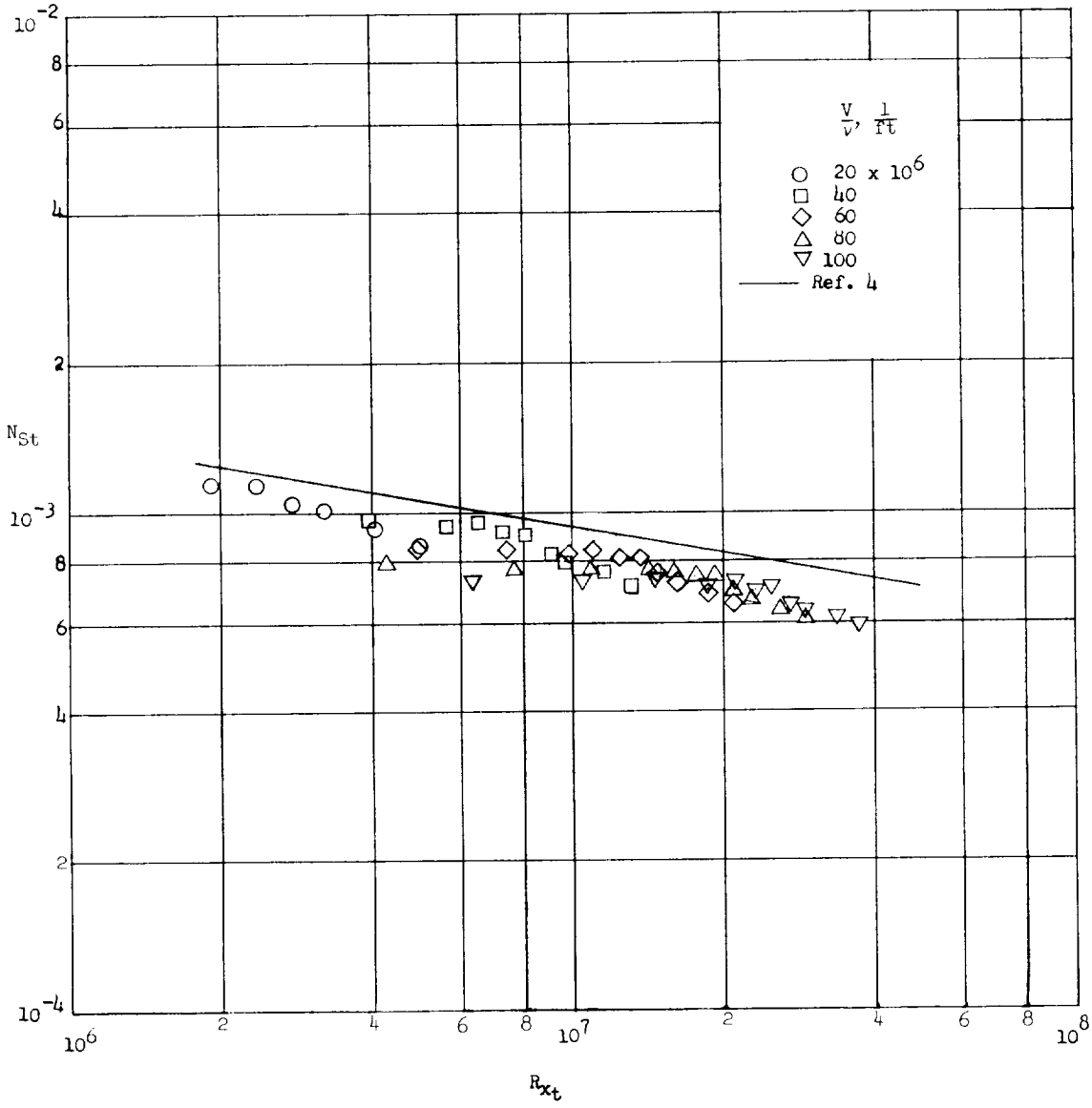

(b) Model 4.

Figure 5.- Concluded.

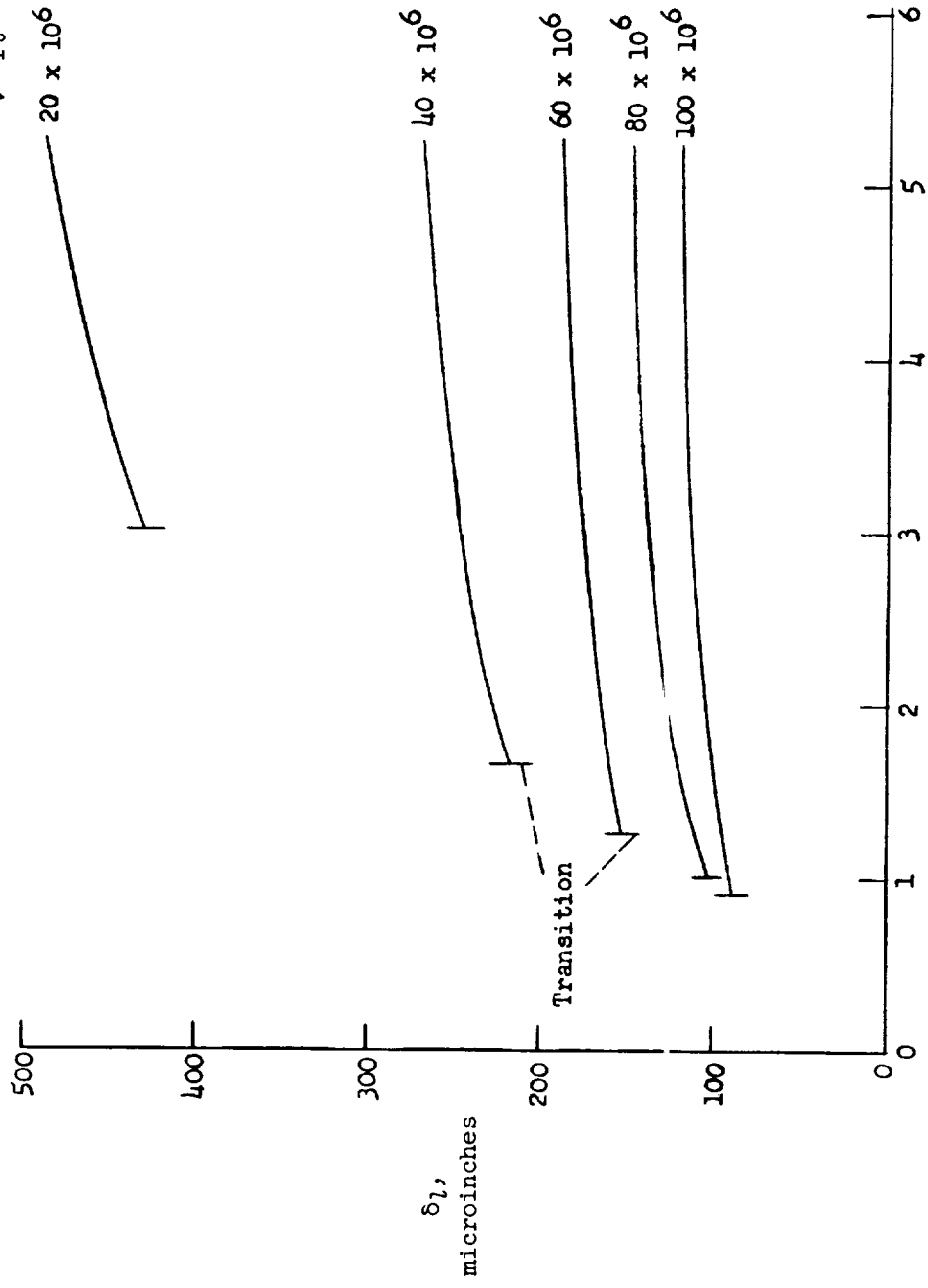

Figure 6.- Thickness of laminar sublayer on model 4.

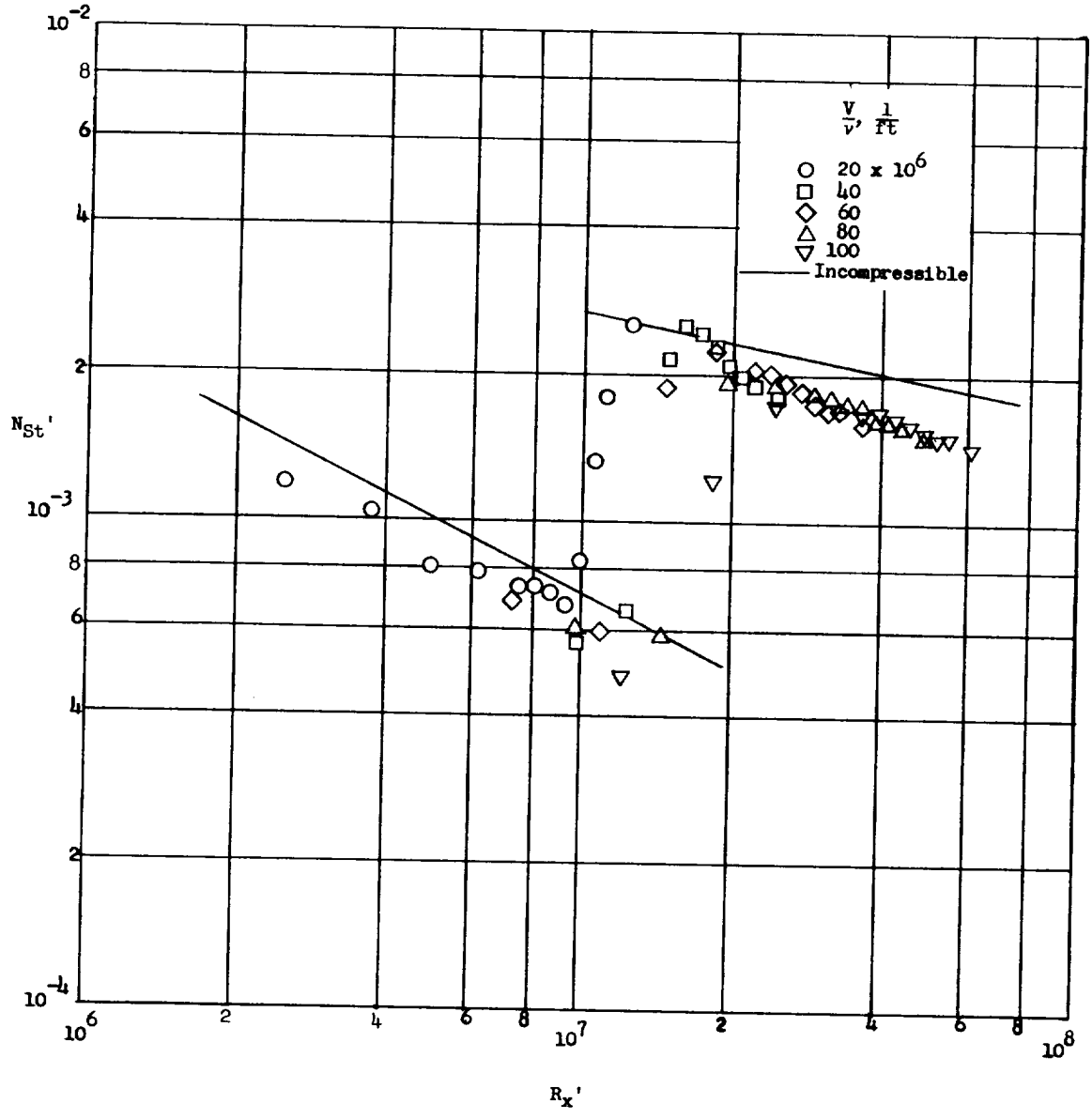

(a) Model 1.

Figure 7.- Heat-transfer data based on reference temperature T'.

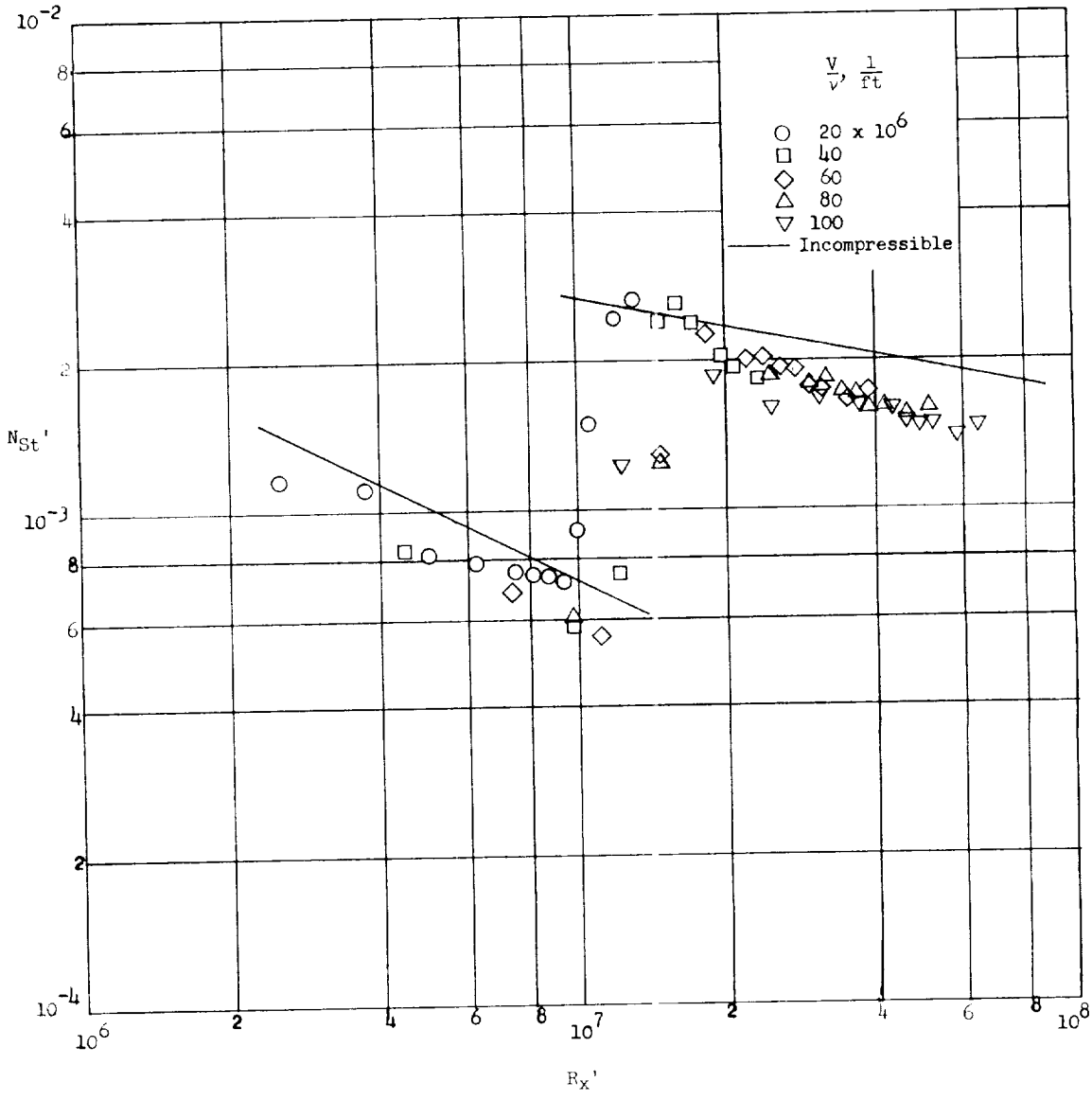

(b) Model 2.

Figure 7.- Continued.

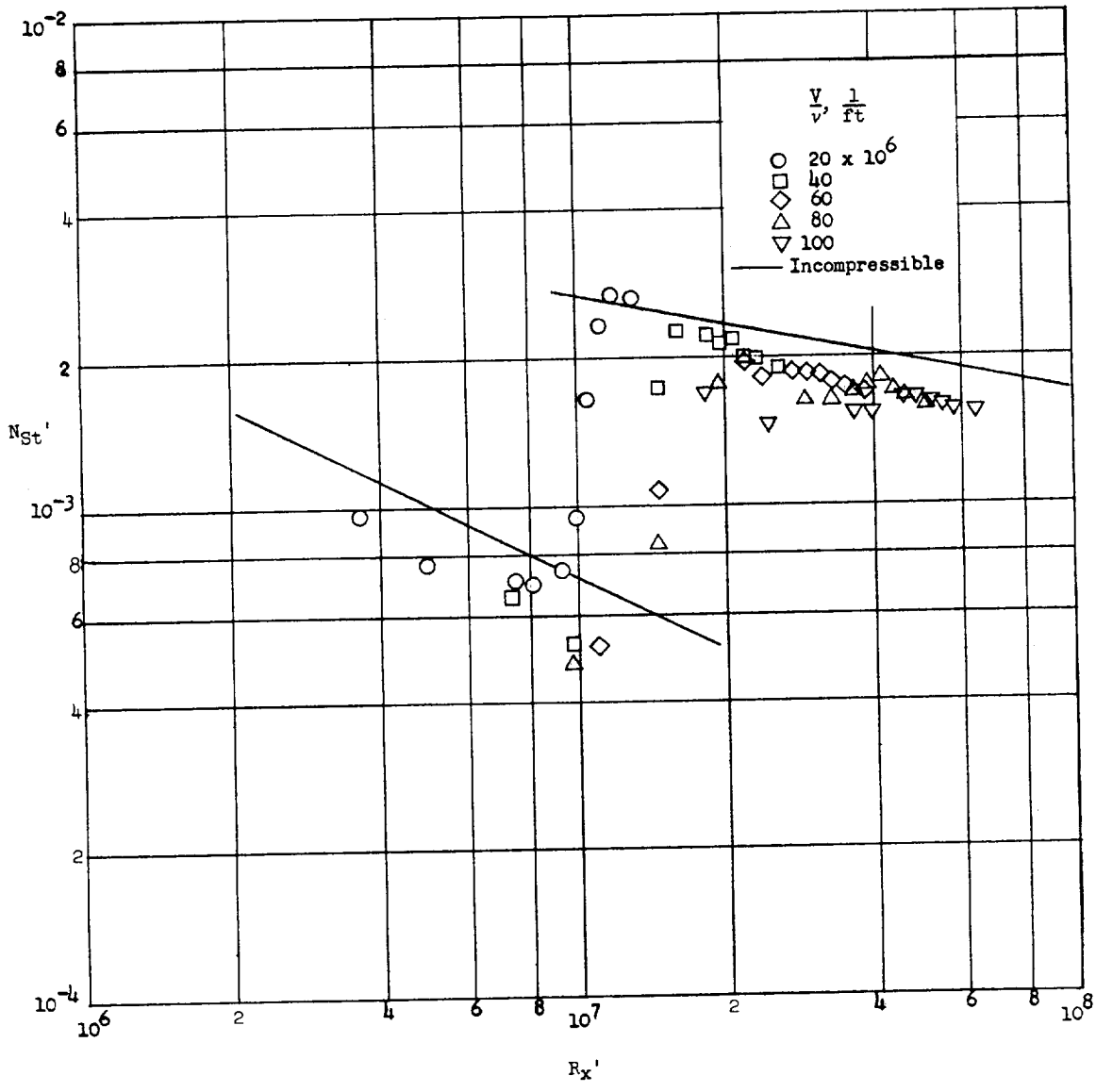

(c) Model 3.

Figure 7.- Continued.

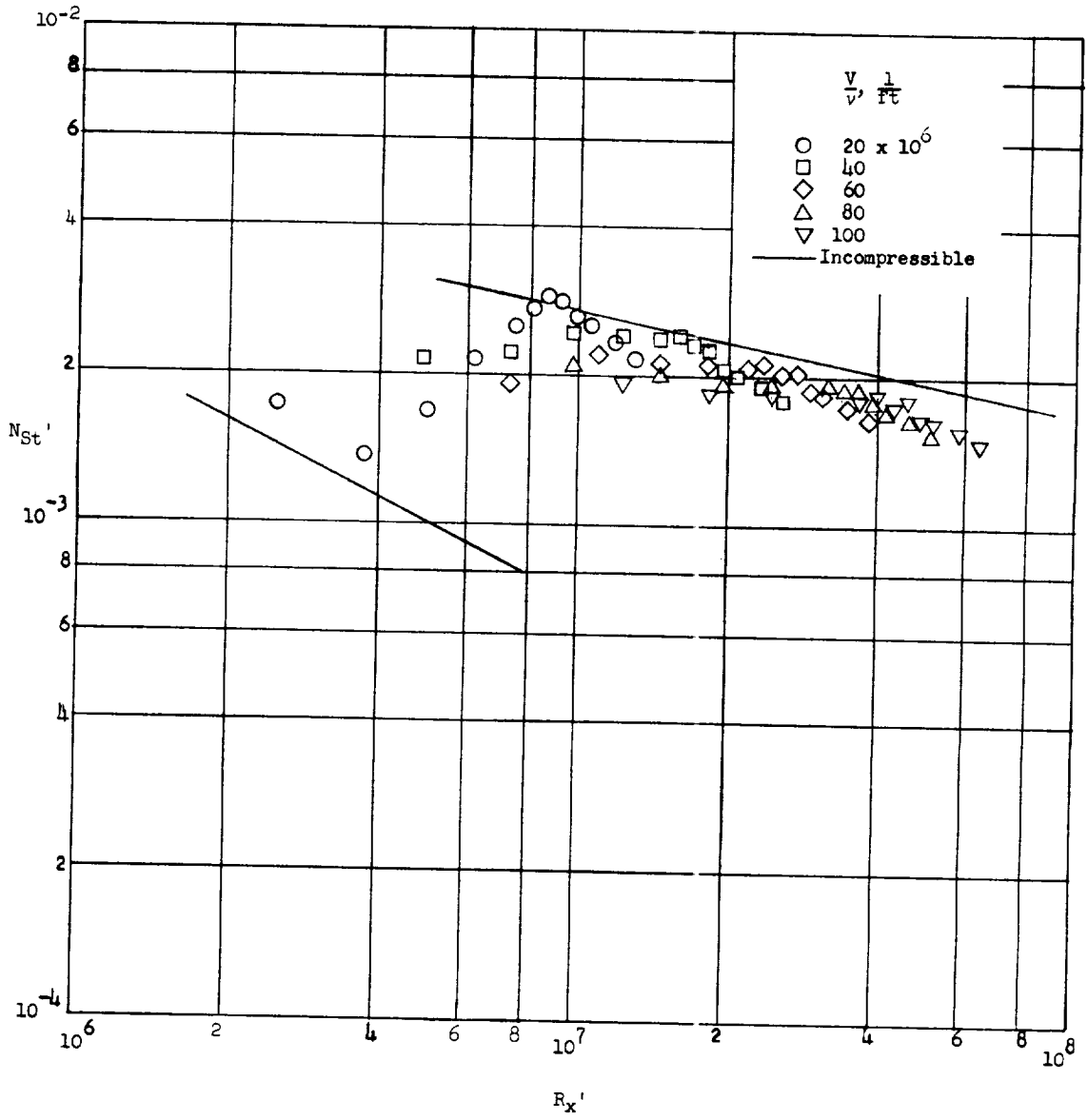

(d) Model 4.

Figure 7.- Concluded.